Systemic Immunologic Consequences of Chronic Periodontitis

D.K. Gaudilliere, A. Culos, K. Djebali, A.S. Tsai, E.A. Ganio, W.M. Choi, X. Han, A. Maghaireh, B. Choisy, Q. Baca, J.F. Einhaus, J.J. Hedou, B. Bertrand, K. Ando, R. Fallahzadeh, M.S. Ghaemi, R. Okada, N. Stanley, A. Tanada, M. Tingle, T. Alpagot, A.J. Helms, M.S. Angst, N. Aghaeepour, and B. Gaudilliere

Supplementary Appendix

Appendix Materials and Methods

Sample Stimulation Conditions

Whole-blood samples collected at baseline (n=28) and three weeks after treatment (n=16) were either left unstimulated or stimulated for 15 minutes at 37°C with one of four stimulation conditions (fig. 1A): *Pg*LPS at 1µg/mL (InvivoGen); IFNα at 100 ng/mL (PBL Assay Science); TNFα at 100ng/mL (PeproTech); or a cytokine cocktail containing IL-2/4/6 and GM-CSF) at 100ng/mL each (BD). Samples were then fixed with proteomic stabilizer (SmartTube Inc.) and stored at $^{-}$80°C until further processing.

Mass Cytometry

Samples were suspended in a hypotonic erythrocyte lysis buffer (SmartTube, Inc.) according to manufacturer instructions. Isolated cells were barcoded as previously described (Behbehani et al. 2014) and stained with a 45-parameter panel for comprehensive characterization of the activity of major immune cell subsets (table S1). Cells were incubated with an iridium-containing intercalator (Fluidigm) overnight at 4°C. Samples were analyzed using the Helios Mass Cytometer (Fluidigm) using normalization beads (Finck et al. 2013) and normalized collectively using Normalizer v0.1 MATLAB Compiler Runtime (MathWorks) (fig. 1B). Files were de-barcoded with a single-cell MATLAB debarcoding tool (Zunder et al. 2015). As our analysis focused on the functional response of each cell type (signaling responses), manual gating was chosen over an unsupervised clustering approach to limit the analysis to the major immune cell subsets, thereby controlling the number of immune features measured and increasing interpretability of results. This selection of cell subsets is also required by the csEN algorithm, which could not be applied with automated gating strategies as the automatically identified clusters are unlabeled and cannot be matched to prior knowledge. Manual gating was performed using Cytobank (fig. S1). A total of 900 immune features were extracted from each blood sample including the frequencies of 18 immune cell subsets representing major innate and adaptive compartments (table S2), their endogenous intracellular signaling activities, and the capacities of each cell

subset to respond to a series of receptor-specific immune challenges including stimulation with *Pg*LPS, IFNα, TNFα and IL-2/4/6 with GM-CSF (fig. 1A).
*Pg*LPS was used as *Pg* is an important bacterium in the local pathogenesis of periodontitis via it's virulence factor LPS, which has been shown to directly trigger signaling responses in a variety of cell types (Kocgozlu et al. 2009). IFNα was used as type I interferons are also necessary for the progression of periodontitis; upregulation of IFN α in periodontitis supports our hypothesis that immune cells in patients with ChP are primed for pro-inflammatory responses (Martin et al. 2001; Mizraji et al. 2017). TNFα was used as it is strongly associated with pathophysiological features of periodontitis, including attachment loss and bone resorption (Graves and Cochran 2003). The cytokine cocktail including IL-2/4/6 and GM-CSF was chosen as IL-2/4/6 are all upregulated in patients with periodontitis (Hegde and Awan 2018; McFarlane and Meikle 1991). The primary goal of our ex-vivo stimulation experiments was to evaluate the integrity of intracellular signaling pathways activated downstream of a subset of inflammatory mediators known to be increased in patients with ChP (including pgLPS, TNFα, IL-2/4/6, GMCSF, and IFNα). Specifically, stimulation experiments with pgLPS, TNFα, IL-2/4/6, GMCSF, and IFNα, respectively test the hypotheses of whether Toll Like Receptor 2/4-, TNF receptor-α, Type I (IL-2/4/6/GMCSF) and Type II (IFNα) cytokine receptor-dependent intracellular signaling responses are differentially regulated in patients with ChP compared to controls. Immune features were derived from measurements performed in whole-blood samples, which allowed the functional assessment of all peripheral immune cell subsets while minimizing perturbations by experimental processing.

Statistical Analysis

Statistical analysis of the mass cytometry data derived from analysis of samples from 28 patients before treatment was performed using the cell-signaling Elastic Net (csEN) method (Aghaeepour et al. 2017); the dataset was complete, with no missing data. A power analysis was not performed for this first exploratory analysis. Briefly, the cell-signaling (cs)EN method developed by Aghaeepour et al., an adaptation of the existing EN regularized regression method, has been shown to significantly outperform the existing EN algorithm (Aghaeepour et al. 2017). The csEN considers previous biological knowledge of cell-type and receptor-specific signaling pathway activation that inherently influences the generation and interpretation of mass cytometry datasets. As such, the csEN prioritizes canonical signaling responses to selected stimulation conditions using a cell signaling-based penalization matrix, such as toll-like receptors 2 and 4 (TLR-2/4) signaling response to *Pg*LPS in innate immune cells and JAK/STAT signaling responses to IFNα in innate and adaptive immune cells, figure 2A and table S2.

We adapted an independently developed cell signaling-based penalization matrix that accounted for whether a cell-type- and receptor-specific signaling response to each stimulation condition is supported by prior knowledge of signal transduction pathways (table S2).

As the csEN has not been previously used to separate patients from controls, it was amended as follows: given a set of immune features, *X*, and a vector classifying participants as "Control" or "Patient", *Y*, a multivariate model is generated by calculating

the coefficients, β, that minimize the negative binomial log-likelihood of the regression model:

$$-\left[\frac{1}{N}\sum_{i=1}^{N} y_i \cdot (\beta_0 + x^T\beta) - \log(1 + e^{(\beta_0 + x^T\beta)})\right]$$

The L1 penalty of the least absolute shrinkage and selection operator (LASSO) (Tibshirani 1996) and L2 penalty of Ridge Regression (Hoerl and Kennard 1970) are added to this calculation by including two hyper parameters λ (the penalization factor) and α (which determines the relative contributions of the penalties):

$$\lambda[\frac{(1-\alpha)\|\beta\|_2^2}{2} + \alpha\|\beta\|_1]$$

Including these penalties in the fitting process allows for both sparsity in the model and inclusion of highly inter-correlated features. To incorporate previous biological knowledge, a scale factor, ϕ, is added to the negative binomial log-likelihood, resulting in the objective function:

$$\mathbf{Eq.\ 1.}\ L(\beta) = -\left[\frac{1}{N}\sum_{i=1}^{N} y_i \cdot (\beta_0 + \phi x^T\beta) - \log\left(1 + e^{(\beta_0 + \phi x^T\beta)}\right)\right] + \lambda[\frac{(1-\alpha)\|\beta\|_2^2}{2} + \alpha\|\beta\|_1]$$

Eq. 1 defines the three parameters (α,λ,ϕ) csEN requires for a binomial regression. The csEN was applied to the baseline mass cytometry dataset. A repeated hold-out method consisting of 4000 repetitions with 22 training observations and six test observations was used to validate the model. For each hold-out instance, parameters were optimized by a gradient-free optimization algorithm which maximizes the Area Under the Recovery Operator Curve (AUROC) during cross-validation of the training samples. A vector of average predictions across each hold-out instance was used in the Wilcoxon rank sum test.

For comparison of csEN model prediction before and after treatment, model coefficients across each hold-out instance were aggregated for projection on samples collected from a subset of patients before and at three weeks after treatment (n=16, Fig. 4). As such, the csEN model trained on baseline immune features from 28 patients provided a unique prediction before and after treatment the study participants that were followed after treatment. These projected values were used during visualization of three-week status. This mean coefficient model was also used for the creation of all related figures.

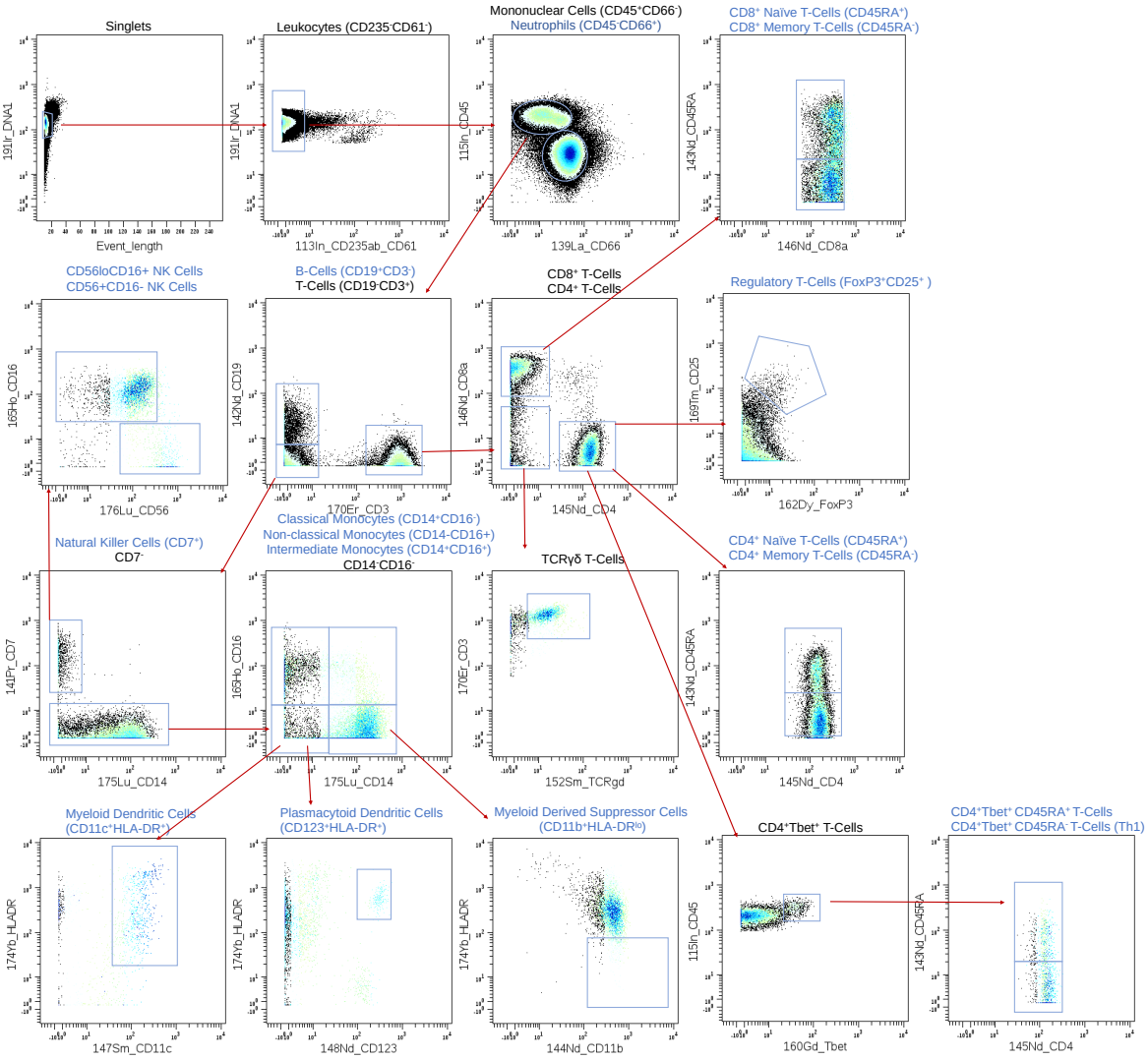

Appendix Figure 1. Gating strategy of immune cell subsets. Two-dimensional mass cytometry plots are shown for a representative patient sample. Gating was performed using Cytobank (www.cytobank.org). Cell types included in the analysis are indicated in blue.

Appendix Table 1. Antibody panel used for mass cytometry analysis

Antibody	Manufacturer	Symbol	Mass	Clone	Comment	Control (mean signal)	ChP (mean signal)
Barcode 1	Trace	Pd	102		Barcode		
Barcode 2	Trace	Pd	104		Barcode		
Barcode 3	Trace	Pd	105		Barcode		
Barcode 4	Trace	Pd	106		Barcode		
Barcode 5	Trace	Pd	108		Barcode		
Barcode 6	Trace	Pd	110		Barcode		
CD235ab*	Biolegend	In	113	HIR2	Phenotype	0.85	0.83
CD61*	BD	In	113	VI-PL2	Phenotype	0.85	0.83
CD45	Biolegend	In	115	HI30	Phenotype	133.18	145.40
CD66	BD	La	139	CD66a-B1.1	Phenotype	96.09	90.35
CD7	BD	Pr	141	M-T701	Phenotype	1.54	1.40
CD19	Biolegend	Nd	142	HIB19	Phenotype	0.74	0.76
CD45RA	Biolegend	Nd	143	HI100	Phenotype	9.31	9.10
CD11b	Fluidigm	Nd	144	ICRF44	Phenotype	295.57	291.33
CD4	Fluidigm	Nd	145	RPA-T4	Phenotype	4.23	4.32
CD8a	Fluidigm	Nd	146	RPA-T8	Phenotype	2.57	2.45
CD11c	Fluidigm	Sm	147	Bu15	Phenotype	20.23	22.62
CD123	Biolegend	Nd	148	6H6	Phenotype	0.37	0.39
pCREB	Cell Signaling	Sm	149	87G3	Function	3.47	3.08
pSTAT5	Fluidigm	Nd	150	47	Function	5.79	5.59
pp38	BD	Eu	151	36/p38	Function	0.22	0.14
TCRγδ	Fluidigm	Sm	152	11F2	Phenotype	0.45	0.45
pSTAT1	Fluidigm	Eu	153	58D6	Function	1.16	1.07
pSTAT3	Cell Signaling	Sm	154	M9C6	Function	2.77	2.88
pS6	Cell Signaling	Gd	155	D57.2.2E	Function	2.50	2.35
CD24	Biolegend	Gd	156	ML5	Phenotype	86.81	95.68
CD38	Biolegend	Gd	157	HIT2	Phenotype	30.67	28.88
CD33	Fluidigm	Gd	158	WM53	Phenotype	7.23	5.64
pMAPKAPK2	Fluidigm	Tb	159	27B7	Function	7.67	7.49
Tbet	Fluidigm	Gd	160	4B10	Phenotype	4.75	4.62
cPARP	BD	Dy	161	F21-852	Function	0.36	0.38
FoxP3	Fluidigm	Dy	162	PCH101	Phenotype	6.05	5.77
IκB	Fluidigm	Dy	164	L35A5	Function	3.60	3.35
CD16	Fluidigm	Ho	165	3G8	Phenotype	153.73	138.98
pNFκB	Fluidigm	Er	166	K10-	Function	4.65	4.68
pERK1/2	Fluidigm	Er	167	D13.14.4E	Function	0.73	0.67
pSTAT6	Fluidigm	Er	168	18	Function	0.60	0.54
CD25	Biolegend	Tm	169	M-A251	Phenotype	0.03	0.02
CD3	Fluidigm	Er	170	UCHT1	Phenotype	1.06	0.87
CD27	BD	Yb	171	M-T271	Phenotype	1.99	1.88
CD15	Fluidigm	Yb	172	W6D3	Phenotype	131.38	142.24
CCR2	Biolegend	Yb	173	K036C2	Phenotype	9.28	9.06
HLA-DR	Fluidigm	Yb	174	L243	Phenotype	1.89	1.95
CD14	Fluidigm	Yb	175	M5E2	Phenotype	0.02	0.03
CD56	BD	Yb	176	NCAM16.2	Phenotype	1.72	1.69
DNA1	Fluidigm	Ir	191		DNA		
DNA2	Fluidigm	Ir	192		DNA		

* CD235ab and CD61 were run on the same metal.

Appendix Table 2. Signaling responses prioritized in the signaling-based penalization matrix

A.

Unstimulated	CREB	ERK	IκB	MK2	NF-κB	P38	S6	STAT1	STAT3	STAT5	STAT6
Nφs	✓	✓	✓	✓	✓	✓	✓	✓	✓	✓	✓
cMCs	✓	✓	✓	✓	✓	✓	✓	✓	✓	✓	✓
ncMCs	✓	✓	✓	✓	✓	✓	✓	✓	✓	✓	✓
intMCs	✓	✓	✓	✓	✓	✓	✓	✓	✓	✓	✓
M-MDSCs	✓	✓	✓	✓	✓	✓	✓	✓	✓	✓	✓
mDCs	✓	✓	✓	✓	✓	✓	✓	✓	✓	✓	✓
pDCs	✓	✓	✓	✓	✓	✓	✓	✓	✓	✓	✓
NK Cells	✓	✓	✓	✓	✓	✓	✓	✓	✓	✓	✓
$CD56^{lo}CD16^{+}$ NK Cells	✓	✓	✓	✓	✓	✓	✓	✓	✓	✓	✓
$CD56^{+}CD16^{-}$ NK Cells	✓	✓	✓	✓	✓	✓	✓	✓	✓	✓	✓
$CD4^{+}$ $T\text{-}Cells_{mem}$	✓	✓	✓	✓	✓	✓	✓	✓	✓	✓	✓
$CD4^{+}$ $T\text{-}Cells_{naive}$	✓	✓	✓	✓	✓	✓	✓	✓	✓	✓	✓
$CD45RA^{-}$ $Tbet^{+}CD4^{+}$ T-Cells	✓	✓	✓	✓	✓	✓	✓	✓	✓	✓	✓
$CD45RA^{+}Tbet^{+}$ $CD4^{+}$ T-cells	✓	✓	✓	✓	✓	✓	✓	✓	✓	✓	✓
Tregs	✓	✓	✓	✓	✓	✓	✓	✓	✓	✓	✓
$CD8^{+}$ $T\text{-}Cells_{mem}$	✓	✓	✓	✓	✓	✓	✓	✓	✓	✓	✓
$CD8^{+}$ $T\text{-}Cells_{naive}$	✓	✓	✓	✓	✓	✓	✓	✓	✓	✓	✓
B-Cells	✓	✓	✓	✓	✓	✓	✓	✓	✓	✓	✓

B.

*Pg*LPS	CREB	ERK	IκB	MK2	NF-κB	p38	S6	STAT1	STAT3	STAT5	STAT6
Nφs	✓	✓	✓	✓	✓	✓	✓				
cMCs	✓	✓	✓	✓	✓	✓	✓				
ncMCs	✓	✓	✓	✓	✓	✓	✓				
intMCs	✓	✓	✓	✓	✓	✓	✓				
M-MDSCs	✓	✓	✓	✓	✓	✓	✓				
mDCs	✓	✓	✓	✓	✓	✓	✓				
pDCs											
NK Cells	✓	✓	✓	✓	✓	✓	✓				
$CD56^{lo}CD16^{+}$ NK Cells	✓	✓	✓	✓	✓	✓	✓				
$CD56^{+}CD16^{-}$ NK Cells	✓	✓	✓	✓	✓	✓	✓				
$CD4^{+}$ $T\text{-}Cells_{mem}$											
$CD4^{+}$ $T\text{-}Cells_{naive}$											
$CD45RA^{-}$ $Tbet^{+}$ $CD4^{+}$ T-Cells											
$CD45RA^{+}Tbe$											

t+ CD4+ T-cells											
Tregs	✓	✓	✓	✓	✓	✓	✓				
CD8+ T-Cells$_{mem}$											
CD8+ T-Cells$_{naive}$											
B-Cells											

C.

IFNα	CREB	ERK	IκB	MK2	NF-κB	p38	S6	STAT1	STAT3	STAT5	STAT6
Nφs								✓	✓	✓	✓
cMCs								✓	✓	✓	✓
ncMCs								✓	✓	✓	✓
intMCs								✓	✓	✓	✓
M-MDSCs								✓	✓	✓	✓
mDCs								✓	✓	✓	✓
pDCs								✓	✓	✓	✓
NK Cells								✓	✓	✓	✓
CD56^{lo}CD16+ NK Cells								✓	✓	✓	✓
CD56+CD16- NK Cells								✓	✓	✓	✓
CD4+ T-Cells$_{mem}$								✓	✓	✓	✓
CD4+ T-Cells$_{naive}$								✓	✓	✓	✓
CD45RA-Tbet+ CD4+ T-Cells								✓	✓	✓	✓
CD45RA+Tbet+ CD4+ T-cells								✓	✓	✓	✓
Tregs								✓	✓	✓	✓
CD8+ T-Cells$_{mem}$								✓	✓	✓	✓
CD8+ T-Cells$_{naive}$								✓	✓	✓	✓
B-Cells								✓	✓	✓	✓

D.

TNFα	CREB	ERK	IκB	MK2	NF-κB	p38	S6	STAT1	STAT3	STAT5	STAT6
Nφs	✓	✓	✓	✓	✓	✓	✓				
cMCs	✓	✓	✓	✓	✓	✓	✓				
ncMCs	✓	✓	✓	✓	✓	✓	✓				
intMCs	✓	✓	✓	✓	✓	✓	✓				
M-MDSCs	✓	✓	✓	✓	✓	✓	✓				
mDCs	✓	✓	✓	✓	✓	✓	✓				
pDCs	✓	✓	✓	✓	✓	✓	✓				
NK Cells	✓	✓	✓	✓	✓	✓	✓				
CD56^{lo}CD16+ NK Cells	✓	✓	✓	✓	✓	✓	✓				
CD56+CD16- NK Cells	✓	✓	✓	✓	✓	✓	✓				

$CD4^+$ $T\text{-}Cells_{mem}$	✓	✓	✓	✓	✓	✓	✓				
$CD4^+$ $T\text{-}Cells_{naive}$	✓	✓	✓	✓	✓	✓	✓				
$CD45RA^-Tbet^+$ $CD4^+$T-Cells	✓	✓	✓	✓	✓	✓	✓				
$CD45RA^+Tbet^+$ $CD4^+$ T-cells	✓	✓	✓	✓	✓	✓	✓				
Tregs	✓	✓	✓	✓	✓	✓	✓				
$CD8^+$ $T\text{-}Cells_{mem}$	✓	✓	✓	✓	✓	✓	✓				
$CD8^+$ $T\text{-}Cells_{naive}$	✓	✓	✓	✓	✓	✓	✓				
B-Cells	✓	✓	✓	✓	✓	✓	✓				

E.

IL-2/4/6, GM-CSF	CREB	ERK	IκB	MK2	NF-κB	p38	S6	STAT1	STAT3	STAT5	STAT6
Nφs		✓						✓	✓	✓	✓
cMCs		✓						✓	✓	✓	✓
ncMCs		✓						✓	✓	✓	✓
intMCs		✓						✓	✓	✓	✓
M-MDSCs		✓						✓	✓	✓	✓
mDCs		✓						✓	✓	✓	✓
pDCs		✓						✓	✓	✓	✓
NK Cells		✓						✓	✓	✓	✓
$CD56^{lo}CD16^+$ NK Cells		✓						✓	✓	✓	✓
$CD56^+CD16^-$ NK Cells		✓						✓	✓	✓	✓
$CD4^+$ $T\text{-}Cells_{mem}$		✓						✓	✓	✓	✓
$CD4^+$ $T\text{-}Cells_{naive}$		✓						✓	✓	✓	✓
$CD45RA^-Tbet^+$ $CD4^+$T-Cells		✓						✓	✓	✓	✓
$CD45RA^+Tbet^+$ $CD4^+$ T-cells		✓						✓	✓	✓	✓
Tregs		✓						✓	✓	✓	✓
$CD8^+$ $T\text{-}Cells_{mem}$		✓						✓	✓	✓	✓
$CD8^+$ $T\text{-}Cells_{naive}$		✓						✓	✓	✓	✓
B-Cells		✓						✓	✓	✓	✓

Appendix Table 3. csEN model immune features, p-value, coefficient. Ranked by p-value.

Stimulation	Cell Type	Signaling Protein	p-value	coefficient
IFNα	$CD8^+$ $T\text{-cells}_{naive}$	pCREB	0.001729	0.028943
***Pg*LPS**	mDCs	pSTAT5	0.001729	0.030384
IL-2/4/6, GM-CSF	$CD56^{lo}CD16^+$ NK Cells	pSTAT1	0.002078	-0.02417
IL-2/4/6, GM-CSF	NK Cells	pSTAT1	0.002486	-0.0144
***Pg*LPS**	ncMCs	pSTAT5	0.002486	0.029313
IL-2/4/6, GM-CSF	NK Cells	pMAPKAPK2	0.004906	-0.02397
TNFα	NK Cells	pMAPKAPK2	0.005761	-0.01478
***Pg*LPS**	$CD8^+$ $T\text{-cells}_{naive}$	pSTAT1	0.006743	0.026939
TNFα	$CD56^{lo}CD16^+$ NK Cells	pMAPKAPK2	0.007866	-0.01512
IL-2/4/6, GM-CSF	$CD56^{lo}CD16^+$ NK Cells	pSTAT6	0.009146	0.015572
IL-2/4/6, GM-CSF	$CD56^+CD16^-$ NK Cells	pMAPKAPK2	0.0106	-0.02112
IL-2/4/6, GM-CSF	$CD56^{lo}CD16^+$ NK Cells	pSTAT3	0.0106	-0.01994
IL-2/4/6, GM-CSF	$Tbet^+CD4^+CD45RA^-$ Tcells	pNF-κB	0.0106	0.024192
IL-2/4/6, GM-CSF	$CD56^{lo}CD16^+$ NK Cells	pMAPKAPK2	0.014108	-0.00887
IL-2/4/6, GM-CSF	pDCs	pMAPKAPK2	0.014108	-0.0179
***Pg*LPS**	cMCs	pSTAT6	0.016203	0.027337
IL-2/4/6, GM-CSF	$CD56^+CD16^-$ NK Cells	pSTAT1	0.018554	-0.00783
IFNα	$CD8^+$ $T\text{-cells}_{naive}$	prpS6	0.018554	0.017136
***Pg*LPS**	cMCs	pSTAT5	0.018554	0.009459
***Pg*LPS**	$Tbet^+CD4^+$ Naïve T-cells	IκB	0.021187	0.017232
IL-2/4/6, GM-CSF	B-cells	pCREB	0.024124	-0.02798
IL-2/4/6, GM-CSF	$CD56^+CD16^-$ NK Cells	pERK	0.024124	-0.01574
IL-2/4/6, GM-CSF	NK Cells	pSTAT3	0.027396	-0.00357
TNFα	$CD56^+CD16^-$ NK Cells	pCREB	0.027396	0.006399
TNFα	Th1 cells	pSTAT6	0.027396	0.022404
***Pg*LPS**	cMCs	pCREB	0.031025	0.01195
***Pg*LPS**	mDCs	pCREB	0.031025	0.016026
IFNα	intMCs	pP38	0.039482	-0.02993
IL-2/4/6, GM-CSF	intMCs	pSTAT1	0.044369	-0.0104
IL-2/4/6, GM-CSF	pDCs	prpS6	0.044369	-0.00693
IL-2/4/6, GM-CSF	$CD4^+T\text{-cells}_{mem}$	IκB	0.049736	-0.02753
***Pg*LPS**	cMCs	pERK	0.049736	0.010535
***Pg*LPS**	cMCs	pNF-κB	0.049736	0.019028
***Pg*LPS**	Grans	pNF-κB	0.049736	0.004326
***Pg*LPS**	M-MDSCs	pERK	0.049736	0.00597
TNFα	B-cells	pCREB	0.049736	-0.00581
TNFα	$CD56^+CD16^-$ NK Cells	pSTAT6	0.049736	-0.01541

Appendix Table 4. Complete Features of Interest.

Stimulation	Cell Type	Activated Protein(s)
***Pg*LPS**	cMCs	STAT6, **CREB↑**, STAT5, **NF-κB↑, ERK↑**
***Pg*LPS**	Grans	**NF-κB↑**
***Pg*LPS**	mDCs	**CREB↑**, STAT5
***Pg*LPS**	M-MDSCs	**ERK↑,** STAT6
***Pg*LPS**	$CD8^+T_{naive}$cells	STAT1
***Pg*LPS**	ncMCs	STAT5
***Pg*LPS**	$CD45RA^+Tbet^+CD4^+$ Tcells	IκB
TNFα	NK Cells	**MAPKAPK2↓**
TNFα	$CD56^+CD16^-$ NK Cells	**CREB↑,** STAT6
TNFα	$CD56^{lo}CD16^+$ NK Cells	**MAPKAPK2↓**
TNFα	B Cells	**CREB↓**
TNFα	$CD45RA^-Tbet^+CD4^+$ (Th1) Cells	STAT6
IFNα	intMCs	p38
IFNα	$CD8^+T_{naive}$cells	CREB, S6
IL-2/4/6, GM-CSF	$CD56^+CD16^-$ NK Cells	**STAT1↓**, MAPKAPK2, **ERK↓**
IL-2/4/6, GM-CSF	B cells	CREB
IL-2/4/6, GM-CSF	$CD56^{lo}CD16^+$ NK Cells	**STAT1↓, STAT3↓**, MAPKAPK2
IL-2/4/6, GM-CSF	intMCs	**STAT1↓**
IL-2/4/6, GM-CSF	$CD4^+$ T_{mem}cells	IκB
IL-2/4/6, GM-CSF	NK cells	**STAT1↓**, **STAT3↓,** MAPKAPK2
IL-2/4/6, GM-CSF	pDCs	S6, MAPKAPK2
IL-2/4/6, GM-CSF	$CD45RA^+Tbet^+CD4^+$ Tcells	NF-κB

Top model features distinguishing patients from controls at baseline (univariate $p < 0.05$). Thirteen features are from LPS stimulation, six are from IFNα stimulation, and 15 are from IL-2/4/6, GM-CSF stimulation. In bold are the 17 features in the cell signaling-based penalization matrix with arrows indicating whether the feature is increased or decreased in patients with ChP compared to controls.

Appendix Table 5. Clinical Correlation

Immune Feature	Clinical Feature	Statistical Test Value	sig*
pMAPKAPK2 in CD56^{lo}CD16^{+}NK Cells in response to TNFα	Periodontal Classification (Stage III vs. IV)	t(12) = 4.62 (higher stage ChP → lower pMAPKAPK2)	0.001*
pCREB in CD56^{+}CD16^{-} NK cells in response to TNFα	Periodontal Classification (Stage III vs. IV)	t(12) = -2.70 (higher stage ChP → higher pCREB)	0.02
pERK in cMCs in response to *Pg*LPS	Missing teeth	r = 0.58, n = 14 (more missing teeth → higher pERK)	0.03
pERK in M-MDSCs in response to *Pg*LPS	Missing teeth	r = 0.60, n = 14 (more missing teeth → more pERK)	0.023
pMAPKAPK2 in CD56^{+} NKcells in response to TNFα	Largest Clinical Attachment Loss	r = 0.56, n = 14 (greater attachment loss → more pMAPKAPK2)	0.037
pSTAT1 in intMCs in response to IL-2/4/6, GM-CSF	Pockets ≥ 5mm	r = -0.53, n = 14 (larger number of pockets → lower pSTAT1)	0.049
pSTAT1 in CD56^{+}NKcells in response to IL-2/4/6, GM-CSF	Radiographic Calculus	r = 0.543, n = 14 (more radiographic calculus → more pSTAT1)	0.045

*Significance assessed at the Bonferroni-corrected α level of 0.0033 corrected for 15 comparisons

Appendix Table 6. Differences in cell frequencies following 15 minute *ex vivo* cytokine stimulation.

Cell Type	Unstim	P. gingivalis	TNFa	IFNa	Cocktail
Neutrophils	52.37 (9.6)	53.42 (8.89)	52.87 (9.6)	52.91 (9.4)	52.81 (9.0)
Classical Monocytes	13.50 (5.8)	12.15 (5.4)	12.65 (5.7)	13.41 (5.7)	12.51 (5.3)
Intermediate Monocytes	0.49 (0.4)	0.30 (0.3)	0.31 (0.3)	0.46 (0.5)	0.43 (0.3)
Non-classical MCs	1.56 (0.7)	1.37 (0.6)	1.37 (0.7)	1.62 (0.7)	1.51 (0.7)
Plasmocytoid Dendritic Cells	0.07 (5.6E-02)	0.08 (5.1E-02)	0.06 (4.4E-02)	0.07 (6.5E-02)	0.04 (4.4E-02)
Myeloid Dendritic Cells	0.47 (1.4)	0.66 (1.3)	0.64 (1.5)	0.48 (1.4)	0.46 (1.2)
$CD56^{+}CD16^{-}$ NK Cells	0.34 (0.7)	0.32 (0.6)	0.34 (0.6)	0.30 (0.6)	0.24 (0.4)
$CD56^{lo}CD16^{+}$NK Cells	6.43 (2.3)	6.63 (2.3)	6.57 (2.2)	6.63 (2.3)	6.32 (2.3)
B Cells	10.38 (4.2)	10.73 (4.3)	10.27 (4.2)	10.09 (4.3)	10.40 (4.5)
$CD4^{+}$ T_{mem} Cells	21.54 (6.5)	22.15 (6.5)	22.01 (6.5)	21.54 (6.4)	22.25 (6.6)
$CD4^{+}$ T_{naive} Cells	15.72 (5.8)	15.56 (5.9)	16.05 (5.9)	15.66 (5.7)	16.45 (5.8)
$CD8^{+}$ T_{mem} Cells	8.13 (3.4)	8.32 (3.3)	8.33 (3.2)	8.29 (3.3)	7.99 (3.3)
$CD8^{+}$ T_{naive} Cells	9.85 (4.4)	10.06 (4.6)	9.93 (4.5)	10.08 (4.4)	10.32 (4.4)
Regulatory T Cells	1.37 (0.4)	1.48 (0.5)	1.57 (0.5)	1.31 (0.4)	1.62 (0.5)

Supplemental References

Aghaeepour N, Ganio EA, McIlwain D, Tsai AS, Tingle M, Van Gassen S, Gaudilliere DK, Baca Q, McNeil L, Okada R et al. 2017. An immune clock of human pregnancy. Sci Immunol. 2(15).

Behbehani GK, Thom C, Zunder ER, Finck R, Gaudilliere B, Fragiadakis GK, Fantl WJ, Nolan GP. 2014. Transient partial permeabilization with saponin enables cellular barcoding prior to surface marker staining. Cytometry A. 85(12):1011-1019.

Finck R, Simonds EF, Jager A, Krishnaswamy S, Sachs K, Fantl W, Pe'er D, Nolan GP, Bendall SC. 2013. Normalization of mass cytometry data with bead standards. Cytometry A. 83(5):483-494.

Graves DT, Cochran D. 2003. The contribution of interleukin-1 and tumor necrosis factor to periodontal tissue destruction. J Periodontol. 74(3):391-401.

Hegde R, Awan KH. 2018. Effects of periodontal disease on systemic health. Dis Mon.

Hoerl AE, Kennard RW. 1970. Ridge regression: Biased estimation for nonorthogonal problems. Technometrics. 12(1):55-67.

Kocgozlu L, Elkaim R, Tenenbaum H, Werner S. 2009. Variable cell responses to p. Gingivalis lipopolysaccharide. J Dent Res. 88(8):741-745.

Martin M, Katz J, Vogel SN, Michalek SM. 2001. Differential induction of endotoxin tolerance by lipopolysaccharides derived from porphyromonas gingivalis and escherichia coli. J Immunol. 167(9):5278-5285.

McFarlane CG, Meikle MC. 1991. Interleukin-2, interleukin-2 receptor and interleukin-4 levels are elevated in the sera of patients with periodontal disease. J Periodontal Res. 26(5):402-408.

Mizraji G, Nassar M, Segev H, Sharawi H, Eli-Berchoer L, Capucha T, Nir T, Tabib Y, Maimon A, Dishon S et al. 2017. Porphyromonas gingivalis promotes unrestrained type i interferon production by dysregulating tam signaling via myd88 degradation. Cell Rep. 18(2):419-431.

Tibshirani R. 1996. Regression shrinkage and selection via the lasso. Journal of the Royal Statistical Society Series B (Methodological). 58(1):267-288.

Zunder ER, Finck R, Behbehani GK, Amir E-AD, Krishnaswamy S, Gonzalez VD, Lorang CG, Bjornson Z, Spitzer MH, Bodenmiller B et al. 2015. Palladium-based mass tag cell barcoding with a doublet-filtering scheme and single-cell deconvolution algorithm. Nat Protoc. 10(2):316-333.